Supplemental Tables

Supplemental Table S1. Oligonucleotide sequences used for the RNAi construct.

name	sequence
ratKCTD6.fwd	GATCCCC CTTCTTACGGACTTCAGAA TTCAAGAGA TTCTGAAGTCCGTAAGAAG TTTTTGGAAC
ratKCTD6.rev	TCGAGTTCCAAAAA CTTCTTACGGACTTCAGAA TCTCTTGAA TTCTGAAGTCCGTAAGAAG GGG

Supplemental Figure Legends

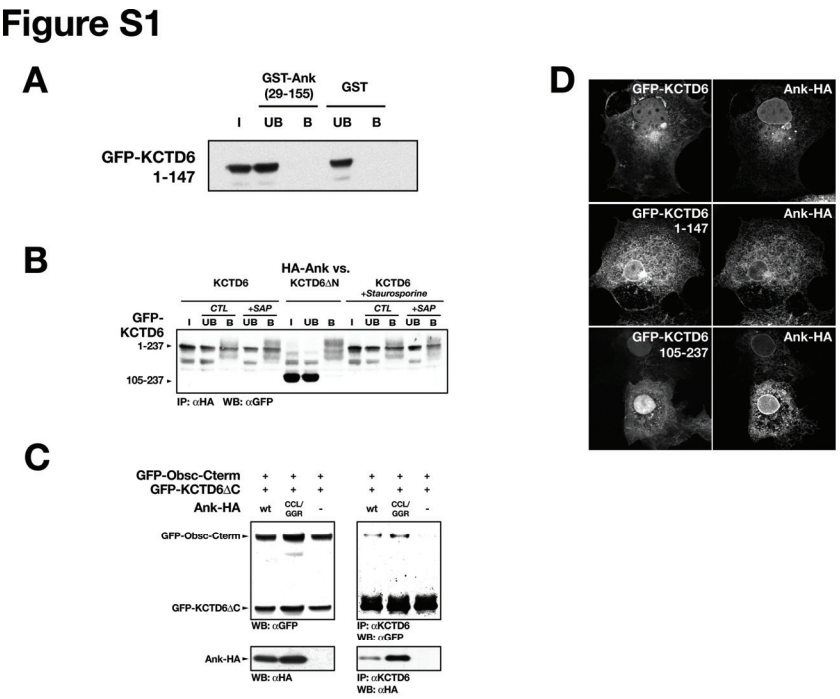

Figure S1. Characterization of sAnk1.5 interaction with KCTD6.

(A) GST-pulldown. Bacterially expressed GST-sAnk1.5 cytoplasmic domain (residues 29-155) shows no affinity for GFP-tagged KCTD6 N-terminus (residues 1-147). GST only serves as negative control. (B) Treatment of transfected differentiated C2C12 cells with staurosporine, or dephosphorylation of proteins isolated from transfected and differentiated C2C12 cells using shrimp alkaline phosphatase (SAP) did not alter interaction of full length KCTD6 with sAnk1.5. KCTD6 C-terminus (residues 105-237) did not interact with sAnk1.5. (C) sAnk1.5, obscurin C-terminus and KCTD6 (1-147) form a ternary complex. Co-immunoprecipitation of KCTD6 (1-147) with sAnk1.5 wildtype or C22G/C34G/L44R triple mutant (that is presumably unable to form oligomeric sAnk1.5 complexes), and obscurin C-terminus indicates that sAnk1.5 is able to interact simultaneously with obscurin and KCTD6. (D) While GFP-KCTD6 N-terminus (residues 1-147) co-localized with HA-tagged sAnk1.5 in transfected COS-1 cells, full length GFP-KCTD6, or KCTD6 C-terminus (residues 105-237) displayed partial or no colocalization with sAnk1.5, respectively. Scale bar 20 μm.

Figure S2

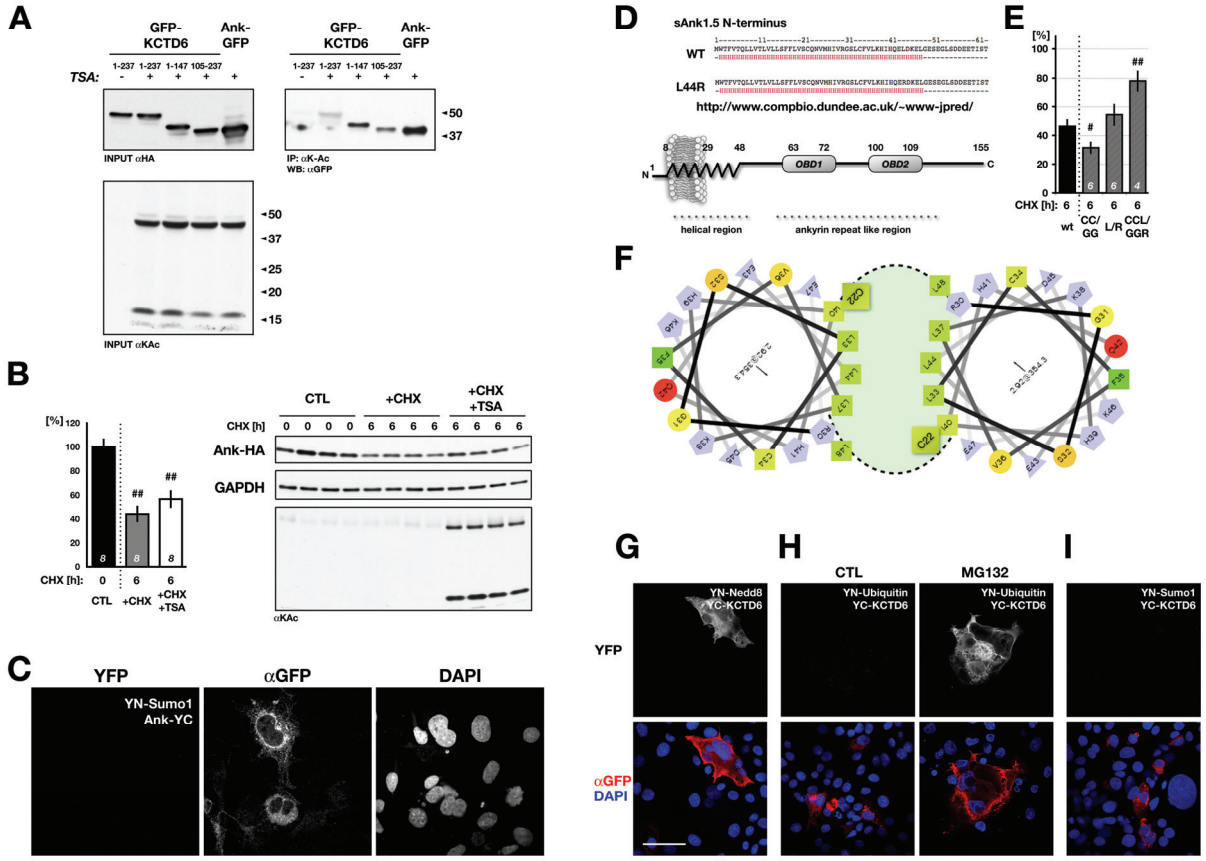

Figure S2. Modification/association of sAnk1.5 and KCTD6 by acetylation, ubiquitin, nedd8 and sumo-1. Influence of sAnk1.5 conformation and oligomerization on protein turnover.

(A) No lysine-acetylation of full length KCTD6. No significant change in lysine acetylation of full length KCTD6 (residues 1-237) can be detected after HDAC inhibition by TSA in transfected Cos-1 cells. Truncated GFP-tagged KCTD6 (residues 1-147 and 105-237), however demonstrated presence of acetylated lysine residues. The positive lysine-acetylation of the truncated KCTD6 may be due to un-associated lysine side-chains that are normally involved in correct folding of full-length protein or formation of KCTD6 oligomers (see Figure S5C). GFP-tagged sAnk1.5 is shown as comparison. (B) Densitometric quantification of HA-tagged sAnk1.5 protein amounts in untreated, and in cells treated for 6 hours with 10µg/ml CHX or 10µg/ml CHX / 0.5µg/ml TSA. ## $p<0.01$ control (CTL) vs. CHX(6); control (CTL) vs. CHX/TSA(6). Note that there is no significant difference between CHX(6) vs. CHX/TSA(6) ($p=0.16$). *n*-values displayed in bottom of bar. Representative images of blots used for densitometric analysis are presented on the right side of this panel. GAPDH was used as loading control. An antibody detecting acetylated lysine residues was used as control for HDAC inhibition. (C) sAnk1.5 is not modified

by small ubiquitin-like modifier sumo-1 in protein complementation assay. (D) Computational analysis of sAnk1.5 secondary structure indicates persistence of sAnk1.5 helical structure to residue 48, well beyond the helical transmembrane domains (residues 8-29). Shown are secondary structure predictions for sAnk1.5 wildtype (WT) and L44R mutant N-terminus. (E) Mutation of cysteine residues in combination with the L44R mutant indicate that disruption of ankyrin oligomerization decreases sAnk1.5 protein degradation (see also Figure 2D-E). Densitometric quantification of wildtype, C22/34G, L44R or C22G/C34G/L44R triple mutant HA-tagged sAnk1.5 protein levels after 6 hours of 10µg/ml CHX treatment. Significant increase or decrease of sAnk1.5 protein degradation was only detectable in C22/34G or triple sAnk1.5 mutant, respectively. * $p<0.05$ vs. wt CHX(0); ** $p<0.01$ vs. wt CHX(0); # $p<0.05$ vs. wt CHX(6); ## $p<0.01$ vs. wt CHX(6); *n*-values for each construct displayed in bottom of bar. (F) Helical pinwheel projection indicates that large hydrophobic residues L33, L37, I40, L44 and L48 orient to one side of the putative sAnk1.5 helical N-terminus. Clustering of this hydrophobic pocket may promote dimerization of sAnk1.5 and orient cystein residues for further oligomerization via disulfide bridge formation.

(G-I) Protein complementation analysis indicates that KCTD6 closely associates with nedd8 (G), ubiquitin (H), but not sumo-1 (I). Cos-1 cells transfected with YC-tagged full length KCTD6 (lower panel, GFP-antibody staining red in overlay) and either YN-tagged nedd8 (G), YN-tagged ubiquitin (H) or YN-tagged sumo-1 (I) display readily detectable association of KCTD6 with nedd8 (G, upper panel). Association of KCTD6 with ubiquitin is only visible after MG132 treatment of Cos-1 cells (H, upper right panel). No association of KCTD6 with sumo-1 was detected (I, upper panel).

Figure S3

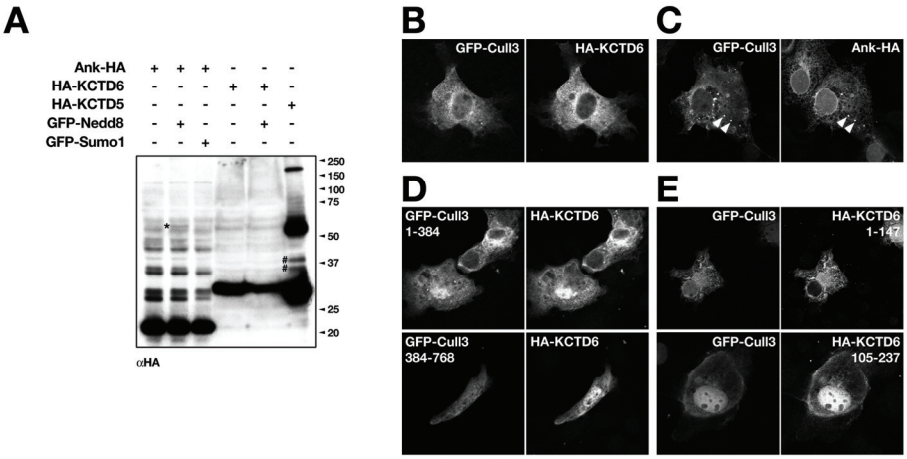

Figure S3. Colocalization of sAnk1.5/KCTD6 complex with cullin-3.

(A) HA-tagged sAnk1.5, KCTD6 and KCTD5 were analyzed in a denaturing SDS-page mobility shift assay. As described before, sAnk1.5 is readily modified by posttranslational modification (Lange *et al.*, 2009). Co-transfection of sAnk1.5 with GFP-tagged nedd8, but not sumo-1 was able to super-shift sAnk1.5 signal (asterisk). In contrast, no additional bands corresponding to presumably neddylated (or ubiquitylated) KCTD6 can be observed in baseline conditions, even upon co-expression with GFP-nedd8. KCTD5 shows additional higher molecular weight bands, some of which are presumably due to posttranslational modification by nedd8 or ubiquitin (hash-tags). Additional high molecular weight bands in KCTD5 may be due to oligomerization (e.g. band at approx. 60kDa). Molecular weight marker in kDa. (B-E) Co-localization of GFP-tagged cullin-3 with either HA-tagged KCTD6 or sAnk1.5 proteins in transfected Cos-1 cells. Cullin-3 co-localizes with KCTD6 (B) and sAnk1.5 (C, arrowheads). (D) N-terminal cullin-3 (residues 1-348) displays better co-localization with KCTD6 (upper panels), compared to C-terminal cullin-3 (residues 384-768; lower panel). (E) Both, KCTD6 N-terminus (residues 1-147) and C-terminus (residues 105-237), display co-localization with cullin-3 in transfected Cos-1 cells. Scale bar 10µm.

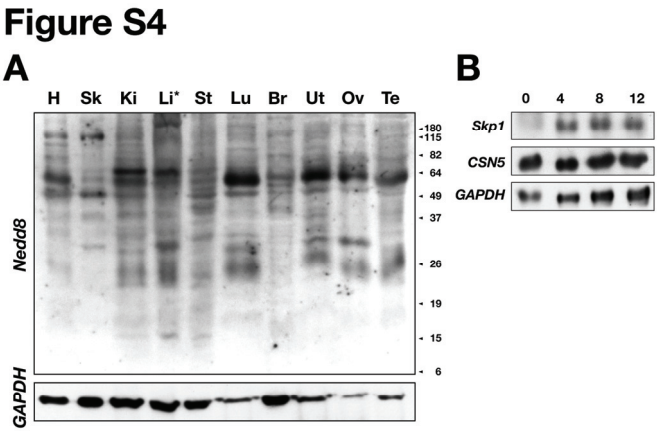

Figure S4. Tissue specific and differentiation profile of Nedd8 and cullin ring ligase associated proteins.

(A) Tissue specific expression profile of nedd8 and neddylated proteins indicate broad expression and modification of Nedd8 and neddylated proteins in all tissues investigated. (B) Analysis of cullin-RING ligase associated proteins Skp1, CSN5, and GAPDH protein levels during C2C12 differentiation. Skp1 displays increased protein levels during C2C12 myotube development, while COP9 signalosome subunit CSN5 remains unchanged.

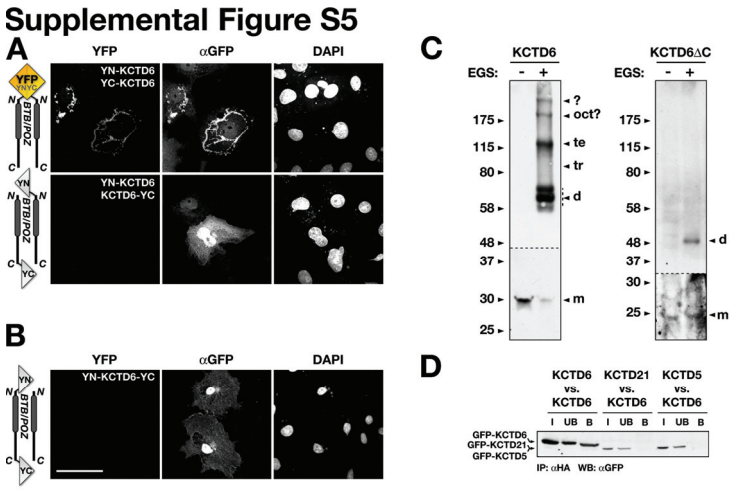

Figure S5. Oligomerization of KCTD6.

(A) Protein complementation assay demonstrates that KCTD6 oligomerizes in parallel fashion. Only transfection of N-terminally tagged KCTD6 construct combinations (YN-KCTD6 + YC-KCTD6, upper panel) show complementation of fluorescent YFP (upper left panel, see also schematic), whereas alternately tagged KCTD6 constructs (YN-KCTD6 + KCTD6-YC, lower panel) fail to show reconstitution of YFP (lower left panel). (B) KCTD6 N-terminus and C-terminus are not in close proximity. Transfection of dual-tagged YN-KCTD6-YC construct into Cos-1 cells failed to show close proximity of KCTD6 N-terminus and C-terminus. (A, B) Scale bar 20μm. (C) Cross-linking of full length HA-tagged KCTD6 (left panel), or KCTD6 N-terminus (residues 1-147, m=monomer; right panel) expressed in COS-1 cells indicates that KCTD6 induces formation of dimers (d) and additional higher molecular weight bands that correspond to KCTD6 tetramers (te), and putatively octamers (oct). Only dimers can be identified when KCTD6 N-terminus was used. Note the presence of three bands at the molecular weight level of the KCTD6 dimer (dotted line). (D) KCTD6 forms only homo-oligomers. Co-immunoprecipitation of HA-tagged KCTD6, with either GFP-tagged KCTD6, KCTD21, or KCTD5 demonstrate that KCTD6 forms only homo-oligomeric complexes. I: input, UB: unbound, B: bound fractions.

Supplemental Figure S6

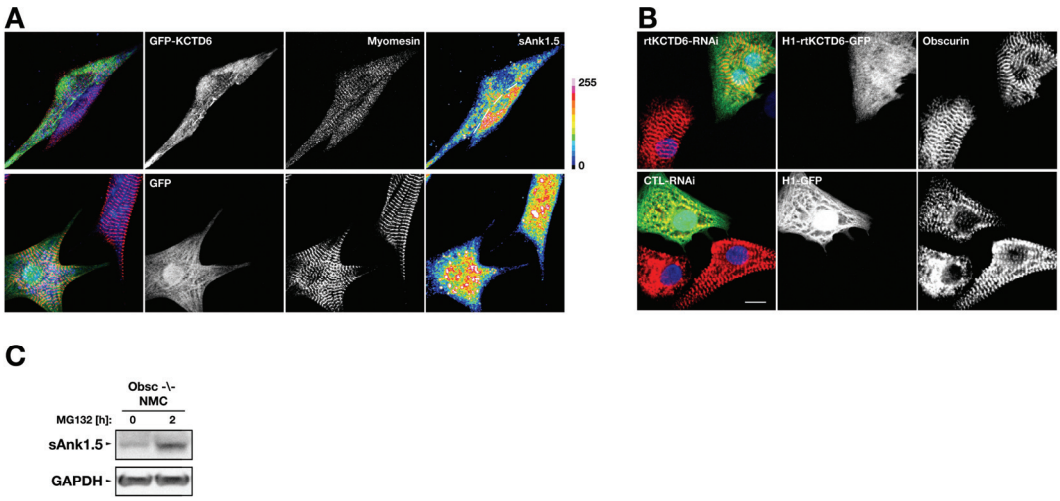

Figure S6. Cellular effects of KCTD6 expression and UPS inhibition.

(A) Transfection of GFP-KCTD6 into neonatal rat cardiomyocytes (NRCs) leads to decreased sAnk1.5 protein levels when compared to GFP transfected (lower panel), or untransfected control cells (right panel, false-color intensity overlay). (B) Knockdown of endogenous KCTD6 in NRC does not disrupt obscurin localization (top panel), similar to H1-GFP controls (bottom panel). (A, B) Scale bar = 10μm. (C) Inhibition of UPS by 20μM MG132 in primary cultures of obscurin knockout neonatal mouse cardiomyocytes for 2 hours leads to increase in endogenous sAnk1.5 protein levels. GAPDH as loading control was unaffected in the observed time-frame.

Supplemental Figure S7

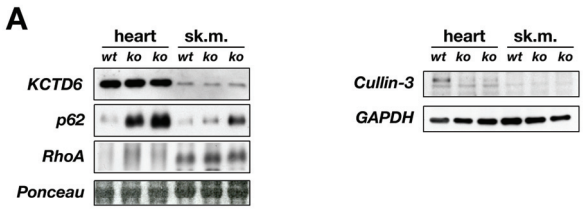

Figure S7. Expression levels of cullin and associated proteins in obscurin knockout muscles.

(A) KCTD6 protein levels are unchanged in muscles from obscurin knockouts, whereas p62 levels increase significantly. Total protein extracts from cardiac and skeletal muscles (tibialis anterior) from wildtype and obscurin knockouts were analyzed with antibodies directed against KCTD6, p62, and RhoA. While KCTD6 and RhoA levels remained unchanged, p62 protein levels are increased in obscurin knockout muscles. Changes to p62 indicate changes to global protein turnover in obscurin knockout cardiac and skeletal muscles. Ponceau staining of actin band is shown as loading control.